DJ Journal of Engineering Chemistry and Fuel, Vol. 2(1) 2017, pp. 1-9

RESEARCH ARTICLE

Binding Interaction study of 5-(difluoromethoxy)-2-Mercapto-1H-Benzimidazole along with $BaTiO_3$ Nanoparticle

R Jayaseelan[1], *M Gopalakrishnan[1]

[1]Department of Chemistry, Annamalai University, Annamalainagar 608 002, India.

Received- 16 September 2016, Revised- 25 November 2016, Accepted- 6 January 2017, Published- 20 January 2017

ABSTRACT

Binding interaction of 5-(difluoromethoxy)-2-mercapto-1H-benzimidazole (DMMB) with $BaTiO_3$ nanoparticle was studied. $BaTiO_3$ nanoparticle was prepared by sol-gel method and characterized by powder X-ray diffraction(XRD). DMMB was loaded on the surfaceof the nanoparticle by adsorption. The interaction of DMMB with $BaTiO_3$ were confirmed by Scanning Electron Microscopy (SEM), Energy- Dispersive X-ray spectroscopy(EDX), Fourier Transform Infrared Spectroscopy (FT-IR), Brunauer-Emmett-Teller (BET), ultraviolet absorption spectroscopy and fluorescence. The results observed proved that the interaction of the DMMB with $BaTiO_3$ occur due to the electron transfer between DMMB and $BaTiO_3$ nanoparticle. DMMB adsorption strongly supports on the surface of $BaTiO_3$ nanoparticle possibly owing to the azomethine nitrogen atom chemical affinity. To confirm the binding of $BaTiO_3$ with DMMB, photo instinct electron transfer is used alongwith fluorescence quenching of DMMB.

Keywords: Imidazole, $BaTiO_3$, XRD, SEM, EDX.

1. INTRODUCTION

Reduced toxicity, less cost, exceptional physicochemical properties and stability of TiO_2 have directed the development of novel TiO_2 based materials, resulting in various implications. Titanium dioxide Nano crystals exhibit in three different phases, viz., anatase, rutile and brookite. The metastable anatase and brookite phases by heating, get converted to rutile phase. These three anatase crystalline phases is photocatalytically reactive and gets prominent implications with their usage. The benchmark photocatalyst TiO_2 P_{25} Degussa, is a rutile (*ca*. 20%) and anatase (*ca*. 80%) blend. TiO_2 is a semiconductor and on illumination with light of energy greater than or equal to the band gap (anatase: 3.2 eV, rutile: 3.0 eV) holes and electrons are produced from the valence and conduction bands, respectively, resulting in photocatalysis [1-10]. $BaTiO_3$ is the number one piezoelectric transducer ceramic ever produced. $BaTiO_3$ is isostructural with perovskite mineral and so is identified as 'a perovskite'. The unit cell is cubic above the Curie Point. The structure is slightly distorted to a tetragonal form along with a dipole moment along the direction below the Curie point. Another transformation develops at the temperatures close to -80 ºC and 0 ºC. Below 0 ºC the unit cell is orthorhombic with the polar axis parallel to a face diagonal. Below -80 ºC it is rhombohedral with the polar axis beside a body diagonal. Likewise the heterocyclic benzimidazole derivatives have brought considerable attention in light luminescence owing to their exclusive optical properties [10] and are employed for making ready functionalized materials [11]. Imidazole nucleus creates the important structure of human organisms, i.e., Vitamin B12, the amino acid histidine and DNA base structure. It also has remarkable analytical applications utilizing their chemiluminescence and fluorescence properties [12-23]. The present investigation explores the adsorption of benzimidazole on the $BaTiO_3$ nanoparticle surface to fine tune the resultant sensor recognition properties.

2. MATERIALS

Barium acetate, Titanium (IV) isopropoxide, which is the chemical and solvent respectively were of analytical grade obtained from commercial suppliers. Solvents were used

*Corresponding author. Tel.: +919442389644
Email address: profmgk61@gmail.com (M.Gopalakrishnan)
Double blind peer review under responsibility of DJ Publications
https://dx.doi.org/10.18831/djchem.org/2017011001

directly without purification. DMMB were purchased from Sigma-aldrich.

3. EXPERIMENTAL

3.1. Synthesis of $BaTiO_3$ by sol-gel method

Barium titanate was obtained by using sol-gel method. $BaTiO_3$ was performed by the chemical polymerization between titanium (IV) isopropoxide and water-soluble barium acetate with 1:1 mole ratio of Ba^{2+}/Ti^{4+} in good acidic atmosphere which is the resulting cause to the formation of barium titanate gel. Then the sample was dried and then calcination treatment of the gel at 700°C was carried out for 2 hrs. The desired barium titanate Nano powder was obtained.

3.2. Surface functionalization of nano $BaTiO_3$

The $BaTiO_3$ nanoparticle surface was introduced by mixing 1.0 g of nano $BaTiO_3$ and 1.0 g of DMMB in 20 ml ethanol. They were vigorously stirred for 3h by using mechanical stirrer. The solid sample was filtered, rapidly washed with ethanol and dried at 100 ºC.

3.3. Measurements

X-ray Diffraction (XRD) pattern of $BaTiO_3$ nanoparticle was recorded, centrifuged and dried using X–ray Rigaku diffractometer with Cu K_α source (30 kV, 100 mA), at a scan speed of 3.0000 deg/min, step width of 0.1000 deg, in a 2θ range of 20-80º. The DMMB interaction with $BaTiO_3$ nanoparticle was observed using UV–Vis spectroscopy by employing a systronics double beam UV–vis spectrophotometer operated on 200–800 nm wavelength. The fluorescence measurements were carried out with Perkin Elmer LS 45 spectrofluorimeter. The Energy Dispersive X-Ray spectra (EDX) of the nanoparticle were recorded with a JEOL JSM-5610 Scanning Electron Microscope (SEM) equipped with Back Electron (BE) detector (EDX) and Energy Dispersive X-ray Spectroscopy (EDX, EDS).The emitted X-rays are quantified as the number of photons vs. energy. The measurement is done using a solid state p-i-n Si (Li) detector, cooled with liquid nitrogen. The sample was placed on a double sided adhesive carbon tape supported on copper stubs and coated with 10 nm thick gold using JEOL JFC- 1600 auto fine sputter coater prior to measurement.

4. RESULTS AND DISCUSSION

4.1. X-ray diffraction pattern of $BaTiO_3$ nanoparticle

The X-ray diffraction pattern of $BaTiO_3$ nanoparticle is shown in figure A1. The most outstanding peaks of $BaTiO_3$ nanoparticle were coordinated with the standard pattern of JCPDS Card No. 31-0174 primitive cubic lattice having crystal constants a = b = 4.034 Aº and c = 4.064 Aº. The average crystalsize (L) of the sol–gel synthesized $BaTiO_3$ has been deduced as 10.44 nm. They have been gaining the full width half maximum of the most intense peaks of the corresponding crystals using the Scherrer equation, $L = 0.9\ \lambda/\beta\cos\theta$, where λ is the X-ray wavelength, θ is the diffraction angle and β is the full width at half maximum of the peak [25].

4.2. Scanning Electron Micrograph (SEM) and EnergyDispersive X-ray spectrum (EDX)

Figure A2 presents the scanning electron micrographs of DMMB adsorbed $BaTiO_3$ nanoparticle and $BaTiO_3$ bare nanoparticle. The SEM image showed that the adsorption of DMMB on $BaTiO_3$ greatly modify the morphology of the $BaTiO_3$ nanoparticle. Figure A3 shows the EDX spectrum of DMMB binding with $BaTiO_3$ nanoparticle and bare $BaTiO_3$ nanoparticle confirm the adsorption of DMMB on $BaTiO_3$ nanoparticle surface.

4.3. Absorption characteristics of DMMB-$BaTiO_3$ nanoparticle

The DMMB absorption spectra in the presence of dispersed $BaTiO_3$ nanoparticle and also in its absence were portrayed in figure A4. The nanoparticle increases the absorbance of DMMB exceptionally without shifting its maximum. This shows that the the excitation technique of DMMB is not altered by the nanocrystal. The enhancement noticedat 262 nm with $BaTiO_3$ nanoparticle is due to DMMB absorption on the $BaTiO_3$ nanoparticle surface. This is due to efficient move of electron from the Excited State (ES) of DMMB to the Conduction Band (CB) of $BaTiO_3$ nanoparticle.

4.4. Fluorescence quenching

Fluorescence spectrum of DMMB and DMMB modified $BaTiO_3$ nanoparticle shown in figure A5. Adding nanoparticle to the DMMB solution resulted in the quenching of its fluorescence emission [24-26]. Azomethine nitrogen was involved in the $BaTiO_3$ nanoparticle binding process. The decrease in fluorescence intensity is associated with the electron transfer between DMMB and $BaTiO_3$ nanoparticle [27, 28]. So the energy transfer was available from the excited state of DMMB to $BaTiO_3$ nanoparticle.

4.5. FT-IR spectral studies

This technique may provide further message about the nature of binding interaction of DMMB with $BaTiO_3$ surface of the nanoparticle. The FT-IRspectra of $BaTiO_3$, DMMB and DMMB-$BaTiO_3$ nanoparticle are displayed in figures A6 and A7. The frequency at 1601 cm^{-1} confirmed to C=N, in the presence of DMMB. This was slightly suppressed in DMMB modified $BaTiO_3$ nanoparticle which clearly revealed the binding of $BaTiO_3$ nanoparticle on azomethine nitrogen of DMMB.

5. CONCLUSIONS

The study of binding interaction of $BaTiO_3$ nanoparticle with DMMB shows the innovative results. SEM with EDX and electronic spectral analysis shows the adsorption of DMMB on the $BaTiO_3$ surface. Enhanced absorption was noted with the dispersed $BaTiO_3$ nanoparticles and are due to the adsorption of DMMB on $BaTiO_3$ surface. Addition of $BaTiO_3$ nanoparticle to the solution of DMMB resulted in fluorescence quenching. The C=N frequency was suppressed at 1613 cm^{-1} and this may be due to the binding of DMMB to the $BaTiO_3$ nanoparticle.

REFERENCES

[1] Rong Wang, Kazuhito Hashimoto, Akira Fujishima, Makota Chikuni, Eiichi Kojima, Atsushi Kitamura Mitsuhide Shimohigoshi and Toshiya Watanabe, Light-Induced Amphiphilic Surfaces, Nature, Vol. 388, 1997, pp. 431-432.

[2] Michael Gratzel, Photoelectrochemical Cells, Nature, Vol. 414, 2001, pp. 338-344.

[3] James S.Reed, Principles of Ceramics Processing, Wiley, New York, 1995, pp. 1-688.

[4] Teruhisa Ohno, Toshiki Tsubota, Maki Toyofuku and Ryoji Inaba, Photocatalytic Activity of a TiO_2 Photocatalyst Doped with C4+ and S4+ Ions Having a Rutile Phase Under Visible Light, Catalysis Letters, Vol. 98, No. 4, 2004, pp. 255-258, http://dx.doi.org/10.1007/s10562-004-8689-7.

[5] Amy L.Linsebigler, Guangquan Lu and John T.Yates, Photocatalysis on TiO_2 Surfaces: Principles, Mechanisms, and Selected Results, Chemical reviews, Vol. 95, No. 3, 1995, pp. 735-758.

[6] Michael R.Hoffmann, Scot T.Martin, Wonyong Choi, Detlef W.Bahnemann, Environmental Applications of Semiconductor Photocatalysis, Chemical reviews, Vol. 95, No. 1, 1995, pp. 69-96, http://dx.doi.org/10.1021/cr00033a004.

[7] N.H.Ince, G.Tezcanli, R.K.Belen and I.G.Apikyan, Ultrasound as a Catalyzer of Aqueous Reaction Systems: the state of the art and environmental applications, Applied Catalysis B: Environmental, Vol. 29, No. 3, 2001, pp. 167-176, http://dx.doi.org/10.1016/S0926-3373(00)00224-1.

[8] Akira Fujishima and Kenichi Honda, Electrochemical Photolysis of Water at a Semiconductor Electrode, Nature, Vol. 238, 1972, pp. 37-38, http://dx.doi.org/10.1038/238037a0.

[9] Marye Anne Fox and Maria T.Dulay, Heterogeneous photocatalysis, Chemical reviews, Vol. 93, No. 1, 1993, pp. 341-357, http://dx.doi.org/10.1021/cr00017a016.

[10] Yoon-Bong Hahn, Rafiq Ahmad and Nirmalya Tripathy, Chemical and Biological Sensors Based on Metal Oxide Nanostructures, Chemical Communications, Vol. 48, No. 84, 2012, pp. 10369-10385, http://dx.doi.org/10.1039/C2CC34706G.

[11] Florentina Maxim, Paula Ferreira, Paula M.Vilarinho and Ian Reaney, Hydrothermal Synthesis and Crystal Growth Studies of $BaTiO_3$ using Ti Nanotube Precursors, Crystal Growth and Design, Vol. 8, No. 9, 2008, pp. 3309-3315, http://dx.doi.org/10.1021/cg800215r.

[12] S.Rezayati, M.T.Jafroudi, E.R. Nezhad, Rahimeh Hajinasiri and Sima Abbaspour, Imidazole-Functionalized Magnetic Fe_3O_4

Nanoparticles: An Efficient, Green, Recyclable Catalyst for One-Pot Friedlander Quinoline Synthesis, Research on Chemical Intermediates, Vol. 42, No. 6, 2016, pp. 5887-5898, http://dx.doi.org/10.1007/s11164-015-2411-9.

[13] A.Mallick, S.C.Bera, S.Maiti and N.Chattopadhyay, Fluorometric Investigation of Interaction of 3-acetyl-4-oxo-6, 7-dihydro-12H indolo-[2, 3-a] quinolizine with Bovine Serum Albumin, Biophysical Chemistry, Vol. 112, No. 1, 2004, pp. 9-14, http://dx.doi.org/10.1016/j.bpc.2004.06.009.

[14] K. Saravanan, N.Srinivasan, V.Thanikachalam and J.Jayabharathi, Synthesis and Photophysics of Some Novel Imidazole Derivatives Used as Sensitive Fluorescent Chemisensors, Journal of fluorescence, Vol. 21, No. 1, 2011, pp. 65-80, http://dx.doi.org/10.1007/s10895-010-0690-5.

[15] C.Karunakaran, J.Jayabharathi and K.Jayamoorthy, Fluorescence Quenching of Organic Molecule by Insulator, Spectrochimica Acta Part A: Molecular and Biomolecular Spectroscopy, Vol. 112, 2013, pp. 417-421, http://dx.doi.org/10.1016/j.saa.2013.04.093.

[16] C.Karunakaran, J.Jayabharathi, R.Sathishkumar and K.Jayamoorthy, Interaction of Fluorescent Sensor with Superparamagnetic Iron Oxide Nanoparticles, Spectrochimica Acta Part A: Molecular and Biomolecular Spectroscopy, Vol. 110, 2013, pp. 151-156, http://dx.doi.org/10.1016/j.saa.2013.03.042.

[17] James G. Wetmur, DNA Probes: Applications of the Principles of Nucleic Acid Hybridization, Critical Reviews In Biochemistry and Molecular Biology, Vol. 26, No. 3-4, 2008, http://dx.doi.org/10.3109/10409239109114069.

[18] Zhixue, Zhou, Yan Du and Shaojun Dong, Double-Strand DNA-Templated Formation of Copper Nanoparticles as Fluorescent Probe for Label-Free Aptamer Sensor, Analytical chemistry, Vol. 83, No. 13, 2011, pp. 5122-5127, http://dx.doi.org/ 10.1021/ac200120g.

[19] David G.Thompson , Alexis Enright , Karen Faulds , W.Ewen Smith and Duncan Graham, Ultrasensitive DNA Detection Using Oligonucleotide−Silver Nanoparticle Conjugates, Analytical chemistry, Vol. 80, No. 8, 2008, pp. 2805-2810, http://dx.doi.org/10.1021/ac702403w.

[20] Chen-Zhong Li, Keith B.Male, Sabahudin Hrapovic and John H.T.Luong, Fluorescence properties of gold Nanorods and their application for DNA biosensing, Chemical Communications, No. 31, 2005, pp. 3924-3926, http://dx.doi.org/10.1039/B504186D.

[21] Xiaogang Li, Meng Meng, Lei Zheng, Zhihuan Xu, Pei Song, Yongmei Yin, Sergei A.Eremin and Rimo Xi, Chemiluminescence Immunoassay for S-Adenosylhomocysteine Detection and Its Application in DNA Methyltransferase Activity Evaluation and Inhibitors Screening, Analytical Chemistry, Vol. 88, No. 17, pp. 8556-8561, http://dx.doi.org/10.1021/acs.analchem.6b01579.

[22] Chockalingam Karunakaran, Jayaraman Jayabharathi, Karunamoorthy Jayamoorthy and Kumar Brindha Devi, Sensing rutile TiO_2 through Fluorescence of Imidazole Derivative, Sensors and Actuators B: Chemical, Vol. 168, 2012, pp. 263-270, http://dx.doi.org/10.1016/j.snb.2012.04.021.

[23] Linlin Wang, Shaopu Liu, Chenxia Hao, Xiaolong Zhang, Chaoqun Wang and Youqiu He, A Dual-Fluorescence Biosensor Assembled by Quantum Dots and Phenazinium Dyes: A Comparative Study for DNA Detection, Sensors and Actuators B: Chemical, Vol. 229, 2016, pp. 145-154, http://dx.doi.org/10.1016/j.snb.2016.01.117.

[24] George J.Kavarnos and Nicholas J.Turro, Photosensitization by Reversible Electron Transfer: Theories, Experimental Evidence, and Examples, Chemical Reviews, Vol. 86, No. 2, 1986, pp. 401-449, http://dx.doi.org/10.1021/cr00072a005.

[25] P.M.Dasami, K.Parameswari, S.Chithra and K.Jayamoorthy, Experimental and Quantum Mechanical Studies on the Corrosion Inhibition of Mild Steel by Quinoline Schiff Bases, DJ Journal of Engineering Chemistry and Fuel, Vol. 1, No. 4, 2016, pp. 1-6, http://dx.doi.org/10.18831/djchem.org/2016041001

[26] C.Karunakaran, J.Jayabharathi, K.Jayamoorthy and P.Vinayagamoorthy, Inhibition of Fluorescence Enhancement of Benzimidazole Derivative on Doping ZnO with Cu and Ag, Journal of Photochemistry and Photobiology A: Chemistry, Vol. 247, 2012, pp. 16-23, http://dx.doi.org/10.1016/j.jphotochem.2012.08.006.

[27] Zhixiang Zhou, Suping Qian, Side Yao and Zhiyi Zhang, Electron Transfer in Colloidal TiO_2 Semiconductors Sensitized by Hypocrellin A, Radiation Physics and Chemistry, Vol. 65, No. 3, 2002, pp. 241-248, http://dx.doi.org/10.1016/S0969-806X(02)00212-8.

[28] Bixia Lin and Zhuxi Fu Yunbo Jia, Green Luminescent Center in Undoped Zinc Oxide Films Deposited on Silicon Substrates, Applied Physics Letters, Vol. 79, No. 7, 2001, pp. 943-945, http://dx.doi.org/10.1063/1.1394173.

APPENDIX A

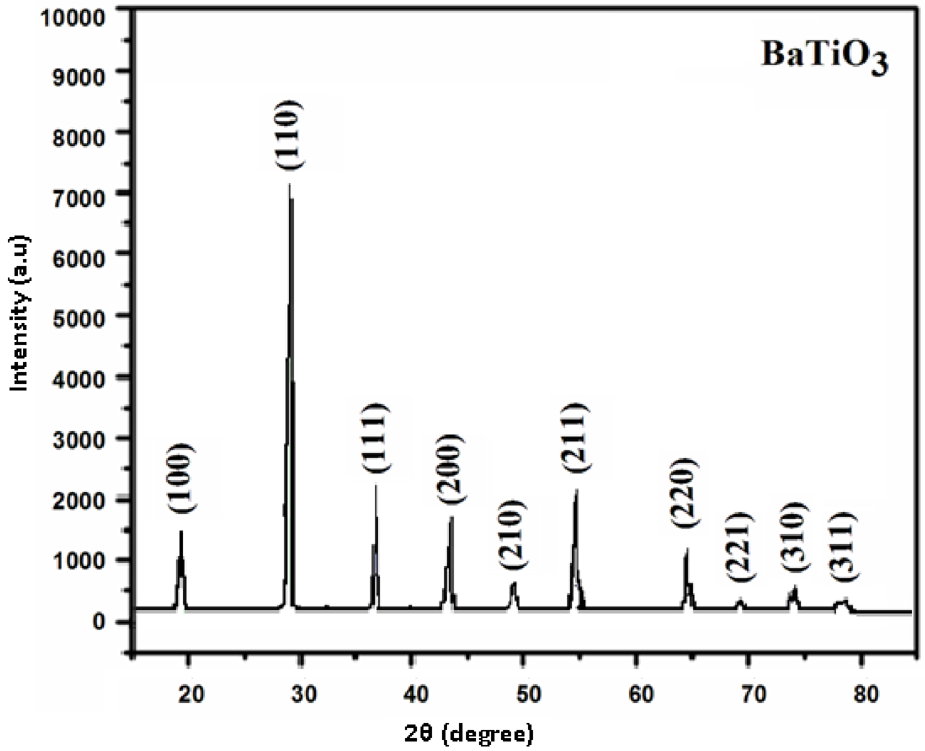

Figure A1.X-ray diffraction pattern of $BaTiO_3$ nanoparticle

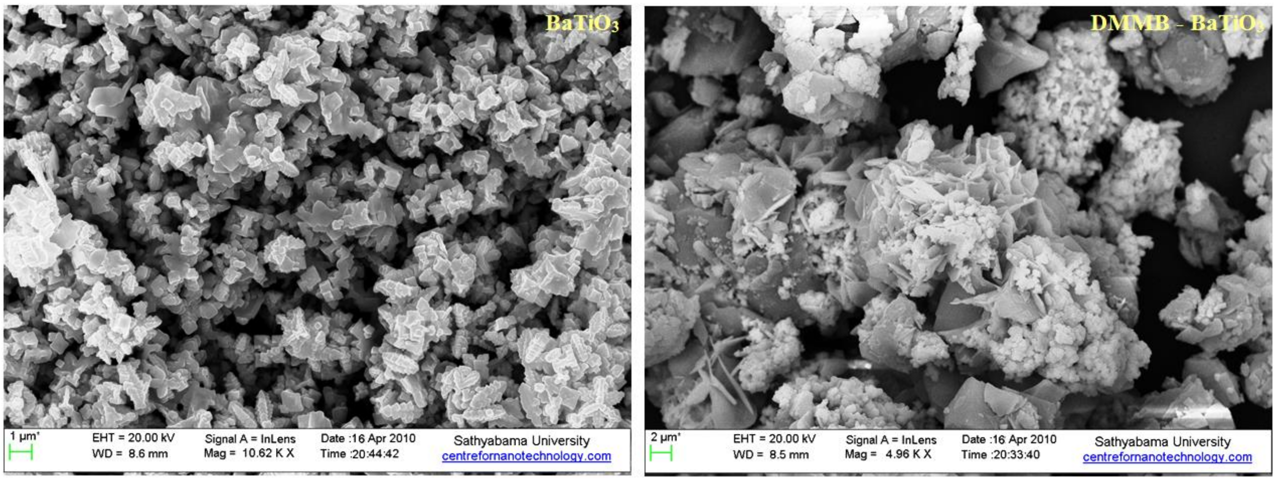

Figure A2.SEM image of imidazole adsorbed $BaTiO_3$ nanoparticle and $BaTiO_3$ nanoparticle

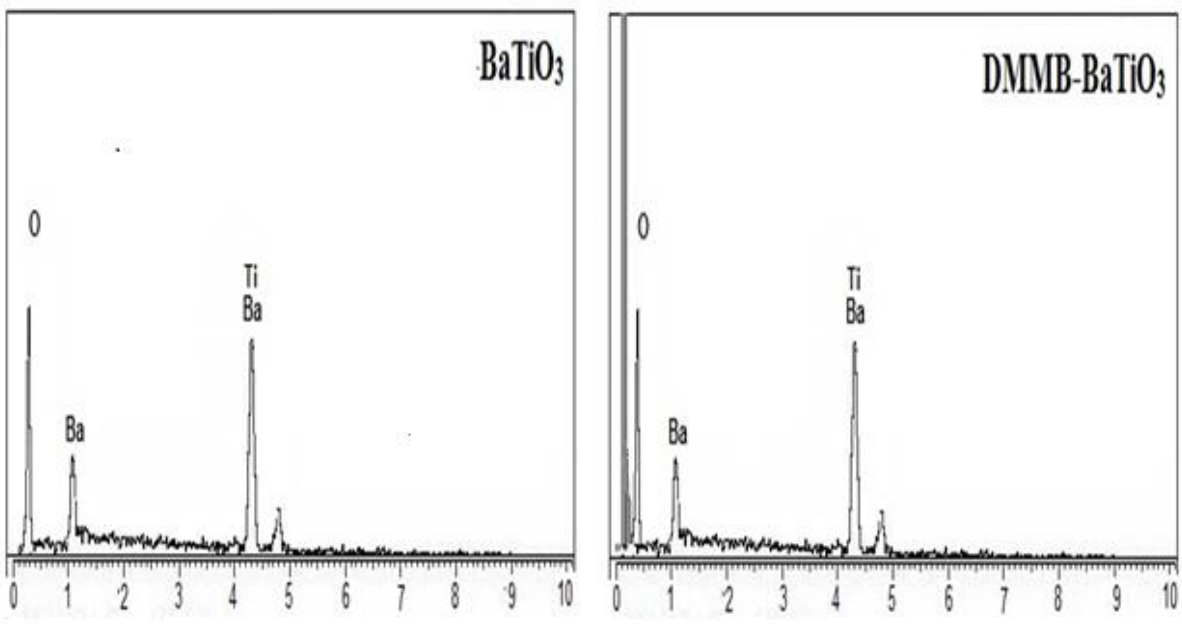

Figure A3.EDX spectrum of imidazole adsorbed $BaTiO_3$ nanoparticle and $BaTiO_3$ nanoparticle

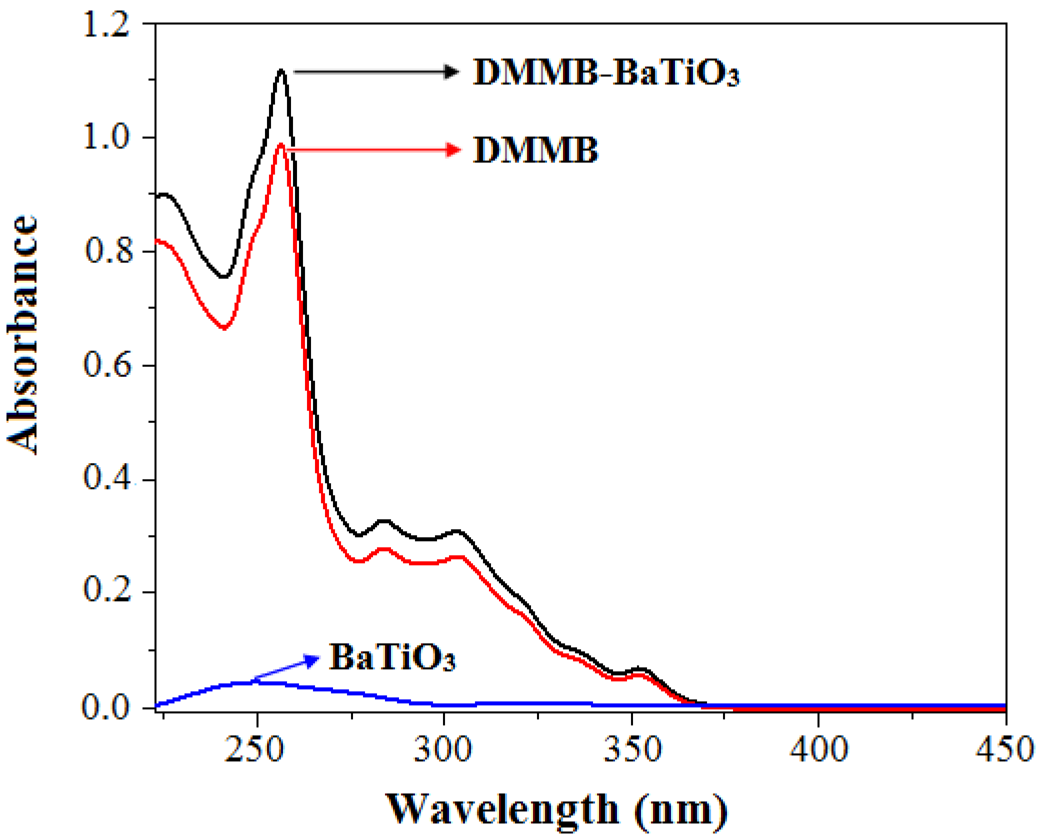

Figure A4.Absorption spectra of imidazole in presence and absence of $BaTiO_3$ nanoparticle.

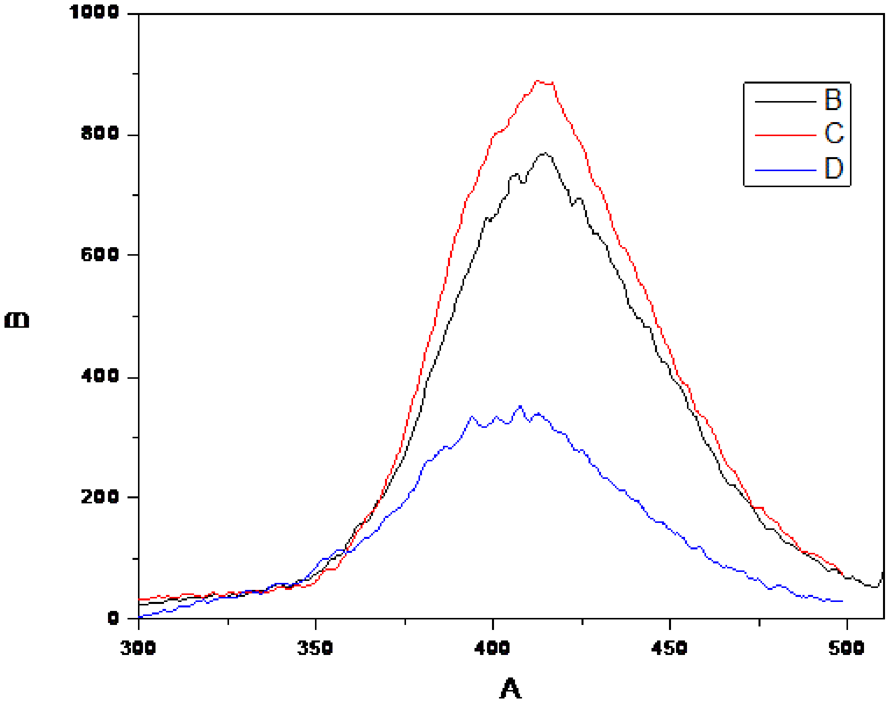

Figure A5.Emission spectra of imidazole in presence and absence $BaTiO_3$ nanoparticle (B, C -imidazole in presence of $BaTiO_3$ nanoparticle; D -imidazole in the absence of $BaTiO_3$ nanoparticle).

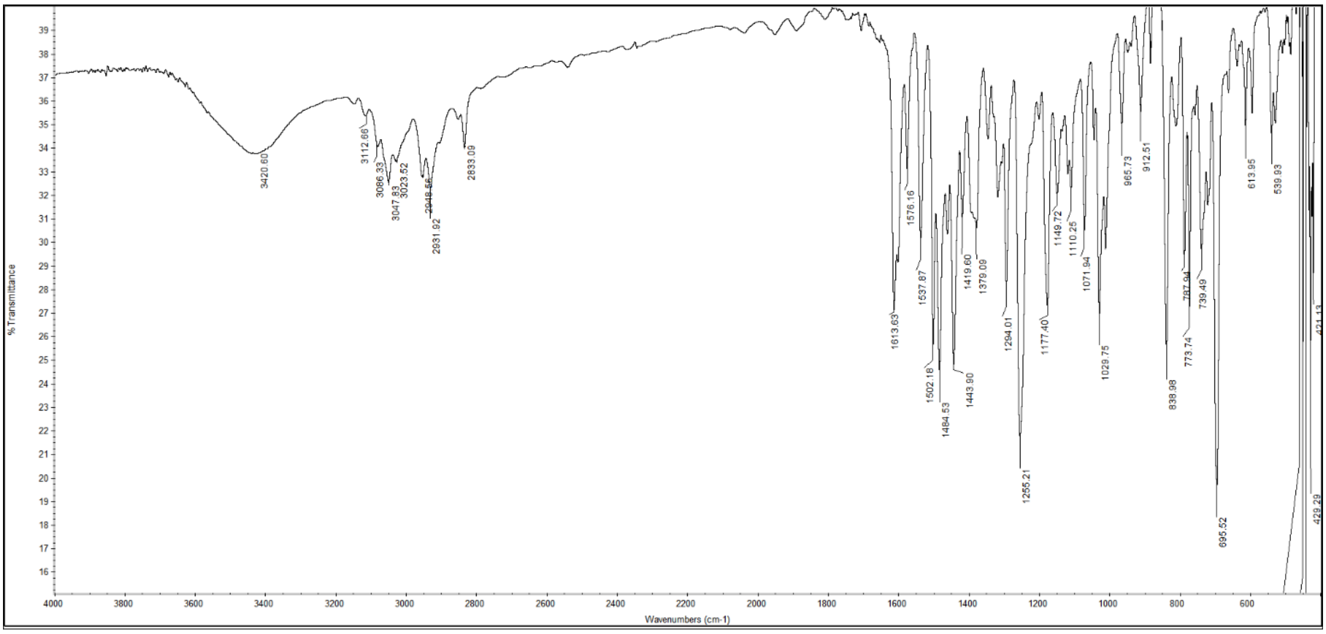

Figure A6.DMMB + $BaTiO_3$ nanoparticle

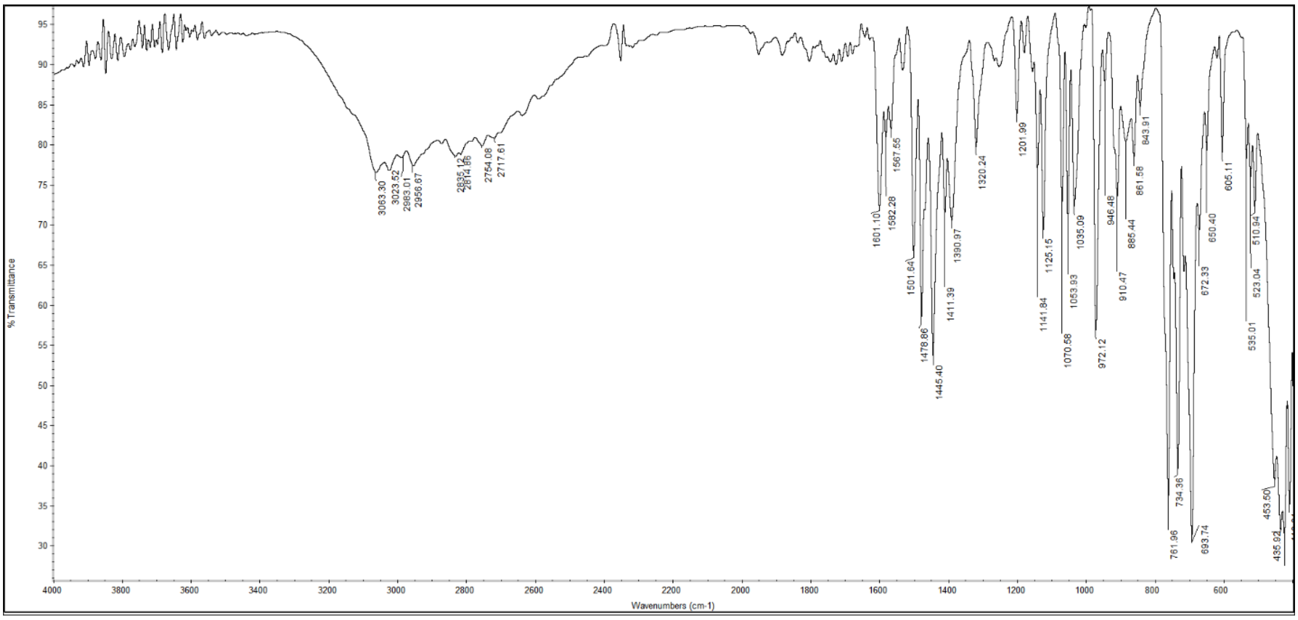

Figure A7.Bare DMMB